Fuel 89 (2010) 1056–1063

Contents lists available at ScienceDirect

Fuel

journal homepage: www.elsevier.com/locate/fuel

Alternative fuel and gasoline in an SI engine: A comparative study of performance and emissions characteristics

Ali M. Pourkhesalian [1], Amir H. Shamekhi *, Farhad Salimi

Mechanical Engineering Department, K.N. Toosi University of Technology, No. 15, Pardis St., MolaSadra Ave., P.O. Box 19395-1999, Vanak Sq., Tehran, Iran

ARTICLE INFO

Article history:
Received 17 January 2009
Received in revised form 16 November 2009
Accepted 17 November 2009
Available online 5 December 2009

Keywords:
Alternative fuels
Emission
Performance
SI engine

ABSTRACT

The strict regulation of environmental laws, the price of oil and its restricted resources, has made engine manufacturers use other energy resources instead of oil and its products. Despite the fact that nowadays alternative fuels are not currently widely used in vehicular applications, using these kinds of fuels will be definitely inevitable in the future. In this paper, a computer code is developed in Matlab environment and then its results are validated with experimental data. This simulated engine model could be used as an powerful tool to investigate the performance and emission of a given SI engine fueled by alternative fuels including hydrogen, propane, methane, ethanol and methanol. Also, the superior of alternative fuels is shown by comparing the performance and emissions of alternative fueled engines to those in conventional fueled engines. Eventually, it is concluded that volumetric efficiency of the engine working on hydrogen is the lowest (28% less that gasoline fueled engine), gasoline produce more power than the all being tested alternative fuels and BSFC of methanol is 91% higher than that of gasoline while BSFC of hydrogen is 63% less than gasoline.

1. Introduction

Alternative fuels are derived from resources other than petroleum. The benefit of these fuels is that they emit less air pollutant compare to gasoline and most of them are more economically beneficial compared to oil and they are renewable. The most common fuels that are used as alternative fuels are natural gas, propane, ethanol, methanol and hydrogen. Lots of works have been done on engine operating with these fuels; few numbers of publications have compared some of these fuels together [1–7]. Majority of previous literatures are comparison between two or three fuels. Verhelst et al. [1] compared a hydrogen/gasoline engine and concluded that the brake thermal efficiency of hydrogen engine exceed than that of gasoline engine. Bayraktar and Durgun [2] has developed and validated an engine simulator to compare performance and emission characteristics of an engine working on LPG and gasoline. Mustafi et al. [3], in their work compared power-gas with gasoline and natural gas (NG). All of the fuel that are discussed in presented paper has widely used as an alternative fuel. Methane, the main content of natural gas (up to 96%), is the most common alternative fuel and is one of the cleanest burning fuels [4]. It can be used in the form of compressed natural gas (CNG) or liquefied natural gas (LNG) to fuel vehicles. Dedicated natural gas vehicles are designed to run on natural gas only. Dual-fuel or bi-fuel vehicles are capable of operating on either gasoline or natural gas. That allows alternative fuel usage which is more economical without sacrificing vehicle operating range and mobility with wide-spread availability of gasoline or diesel [4]. Ethanol and methanol are alcohol-based fuels made by fermenting and distilling starch crops, such as corn. Both ethanol and methanol produce less emission than gasoline [5]. In Brazil, ethanol is well known as a clean, economic and available fuel for vehicles. But engines work on alcoholic fuels will experience a decrement in brake torque and power compared to gasoline [5].

Propane or liquefied petroleum gas (LPG) is a clean-burning fuel that can be used to power internal combustion engines (ICEs). LPG-fueled vehicles produce fewer toxic and smog-forming air pollutants. LPG is usually less expensive than gasoline [2].

Hydrogen (H_2) is an attractive alternative energy carrier. It is being widely investigated as a fuel for passenger car. It can be used in fuel cells to power electric motors or burned in ICEs. Hydrogen produces no air pollutants or greenhouse gases when used in fuel cells and it produces only NOx emission when burned in ICEs [6,7].

In this paper, a detailed comparison between more conventional alternative fuels has been performed. For this purpose, engine performance and exhaust emissions have been experimentally studied for gasoline, methane and methanol in a wide range of engine operating conditions. For other fuels, a thermodynamic model of an SI engine in Matlab environment has been

* Corresponding author. Tel.: +98 21 84063246; fax: +98 21 88677273.
E-mail addresses: pourkhesalian@yahoo.com (A.M. Pourkhesalian), shamekhi@kntu.ac.ir (A.H. Shamekhi), salimi84@yahoo.com (F. Salimi).
[1] Tel.: +98 912 1045151; fax: +98 21 88579480.

0016-2361/$ - see front matter © 2009 Elsevier Ltd. All rights reserved.
doi:10.1016/j.fuel.2009.11.025

Nomenclature

Symbols

A/F	air to fuel
A	area (m^2)
A_R	reference area (m^2)
atm	atmosphere
C_D	discharge coefficient
c_p	specifics heat at constant pressure (J/kg K)
c_v	specific heat at constant volume (J/kg K)
D_v	valve diameter (mm)
e	specific energy (kJ/kg)
E	energy (J)
h	special enthalpy (J/kg)
hp	horse power (hp)
L_V	valve lift (mm)
m	mass (kg)
m_l	leakage mass (due to blowby) (kg/s)
$\dot{m}$	mass flow rate (kg/s)
NOx	nitric oxides
P	pressure (Pa)
P_0	stagnation pressure (Pa)
Pb	brake power (hp)
P_T	pressure at the restriction (Pa)
Q	heat transfer (J)
R	gas constant (kg/kJ K)
T	temperature (K)
V	volume (m^3)
u	burning velocity (m/s)
u'	root mean square turbulent velocity (m/s)
W	work transfer (J)
$\overline{U}_P$	mean piston speed (m/s)
α_T	temperature exponent
β_P	pressure exponent
ϕ	fuel to air equivalence ratio
θ	crank angle (°)
γ	specific heat ratio
ρ	density (kg/m^3)

Acronyms

ABDC	after bottom dead centre
ATDC	after top dead centre
BDC	bottom dead centre
BBDC	before bottom dead centre
BMEP	brake mean effective pressure
BSFC	brake specific fuel consumption
BSNOx	brake specific NOx
BTDC	before top dead centre
CA	crank angle
CI	compression ignition
CNG	compressed natural gas
ECU	electronic control unit
EVO	exhaust valve opening
EXP	experimental
ICE	internal combustion engine
IVO	intake valve opening
LNG	liquefied natural gas
LPG	liquefied petroleum gas
RON	research octane number
RPM	revolution per minute
SA	spark advance
TDC	top dead centre
SI	spark ignition
PPM	particles per million

Subscripts

0	reference condition
b	burned
f	flame
l	laminar
t	turbulent
u	unburned

developed and validated. As combustion of each fuel has its own characteristics, the code has to be modified for each fuel. For estimating the turbulent flame speed, different methods have been used. The code has the ability of evaluating performance and emission characteristics, such as break power, brake torque, brake mean effective pressure, volumetric efficiency, NOx and CO concentrations. The simulation results show good correlation with experimental data.

2. Experimental setup

Experiments were carried out on a four cylinder Mazda B2000i engine. The engine is four-stroke, four-cylinder, spark ignition and naturally aspirated. Bore and stroke are both 86 mm, connecting rod length is 153 mm and compression ratio is 8.6. It has three valves per cylinder. Maximum power is 70 kw at 5000 rpm and maximum torque is 151 Nm at 2500 rpm. Intake valve opening and closing take place at 10 BTDC and 49 ABDC, respectively. Also, exhaust valve opening and closing take place at 55 BBDC and 12 ATDC, respectively.

The test engine was coupled to an eddy-current dynamometer for measuring engine speed and load. Dynamometer Type is Ricardo FE 760-S. Maximum power, torque and engine speed that can be measured by the dynamometer are: 191.17 kw, 610 Nm and 12,000 rpm, respectively. The layout of the experimental setup is shown in Fig. 1. The test engine is converted from a gasoline engine (Mazda B2000i) to a bi-fuel (CNG + gasoline) engine and equipped with a suitable bi-fuel system. In order to achieve desired data, sensors were mounted in suitable positions.

In-cylinder pressure data was taken by a Kistler 6117B piezoelectric high-pressure transducer. The crank shaft position was measured by a Kistler 2613B with a resolution of 1 degree of crank angle (CA). Emission data were taken using a Pierburg HGA 400 exhaust gas analyzer. Air/fuel ratio was monitored by a HORIBA lambda analyzer. Emerson micro motion elite sensor and AVL 753 fuel mass flow meter were used to measure the mass and temperature of injected fuel. Tests have been done for gasoline, methane and methanol under engine steady state conditions. For engine running on methane, a CNG kit was installed. The CNG kit used in the tests was PRINS (VSI). Also a CNG storage tank was used [4]. Fuels properties that have been used in presented research are listed in Table 1.

Data were collected simultaneously from sensors and sent to a data acquisition system. Also, data from engine torque and exhaust gases were recorded which included the concentration of NOx, total unburned hydrocarbons (THC), CO, CO_2 and O_2 in exhaust emissions. Electronic control unit (ECU) data such as injection time, injection duration and spark advance were monitored by Mazda OBD II device [4].

3. Modeling

The engine model is a quasi-dimensional two-zone model including ordinary differential equations for describing dynamical

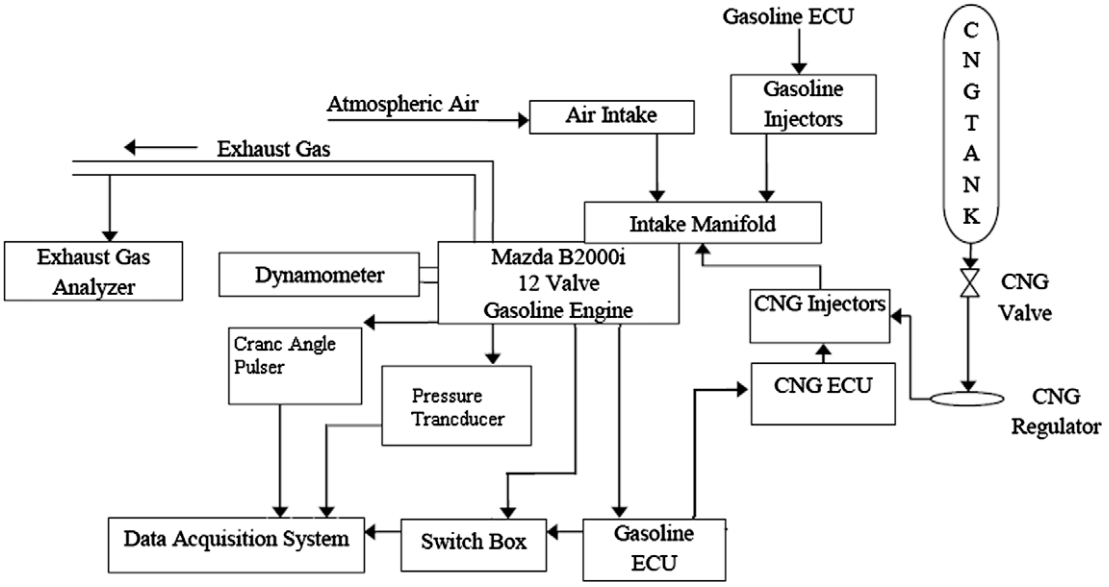

Fig. 1. Experiment layout.

Table 1
Fuels properties [8].

Fuel type	RON	Formula	Molecular weight	Density (kg/m^3)	Heat of vaporization at 298 K (kJ/kg)	Lower heating value (MJ/kg)	Stoichiometric air/fuel ratio
Gasoline	95.8	$C_{7.56}H_{15.5}$	106.22	750	305	44.0	14.6
Methane	120	CH_4	16.04	720	–	50.0	17.23
Methanol	106	CH_4O	32.04	792	1103	20.0	6.47
Ethanol	107	C_2H_6O	46.07	785	840	26.9	9.00
Propane	112	C_3H_8	44.10	545	426	46.4	15.67
Hydrogen	106	H_2	2.015	90	–	120.0	34.3

behavior during the intake, compression, power and exhaust strokes. In this model, the combustion chamber is divided into two zones by flame front. First zone contains unburned and the second one contains burned mixture. Thermal NOx formation also takes place in burned zone, which is modeled by the extended Zeldovich mechanism [8]. The flame front is assumed to travel by turbulent flame speed which is a function of laminar flame speed. The engine model uses Woschni correlation [9] to estimate engine heat transfer. It is assumed that the flame travels in a sphere like shape. The engine model also includes a friction model to predict brake mean effective pressure. The frictional processes in an internal combustion engine can be categorized into three main components: The mechanical friction, the pumping work and the accessory work. For this work, a method which calculates the total friction work accurately, was used [10]. The applied friction model predicts all the categories above. The composition of the reaction products is calculated from the chemical equilibrium at a given pressure and temperature of the 12 species; including: N_2, NO, N, CO_2, CO, OH, H, O_2, O, H_2O, H_2, Ar. Finally, using Newton–Raphson method, molar fraction of each species and total mole fraction was calculated [11].

3.1. Model formulation

The basic equation for the engine model that is derived from first law of thermodynamics is:

$$dE = -\delta Q - \delta W + \sum_i h_i dm_i \tag{1}$$

where E is the internal energy of the cylinder gas mixture, Q is the heat exchange of the cylinder contents with the cylinder walls, W is the work, h_i is the specific enthalpy of gas which enters or leaves the cylinder, and dm_i is the mass flow into (+) or out of (−) the cylinder. δW can be expressed as $P.dV$, where P is the pressure and V is the cylinder volume [8].

3.1.1. Intake and exhaust strokes

The mass flow rate through a valve is usually described by the equation for compressible flow through a flow restriction. This equation is derived from a one-dimensional isentropic flow analysis, and real gas flow effects are included by means of an experimentally determined discharge coefficient, C_D. The air flow rate is related to the upstream stagnation pressure, $P_\circ$ and stagnation temperature, $T_\circ$ static pressure just downstream of the flow restriction (assumed equal to the pressure at the restriction, P_T), and a reference area A_R characteristic of the valve design [8]:

$$\dot{m} = \begin{cases} \frac{C_D A_R P_\circ}{(RT_\circ)^{\frac{1}{2}}} \left(\frac{P}{P_\circ}\right)^{\frac{1}{\gamma}} \left\{ \frac{2\gamma}{\gamma-1} \left[1 - \left(\frac{P_T}{P_\circ}\right)^{\frac{(\gamma-1)}{\gamma}} \right] \right\}^{\frac{1}{2}} & \text{if } \frac{P_T}{P_\circ} > \left[\frac{2}{(\gamma+1)}\right]^{\frac{\gamma}{(\gamma-1)}} \\ \frac{C_D A_R P_\circ}{(RT_\circ)^{\frac{1}{2}}} \gamma^{\frac{1}{2}} \left(\frac{2}{\gamma+1}\right)^{\frac{(\gamma+1)}{2(\gamma-1)}} & \text{if } \frac{P_T}{P_\circ} \leqslant \left[\frac{2}{(\gamma+1)}\right]^{\frac{\gamma}{(\gamma-1)}} \end{cases} \tag{2}$$

For flow into the cylinder through an intake valve, $P_\circ$ is the intake pressure and P_T is the cylinder pressure. For flow out of the cylinder through an exhaust valve, $P_\circ$ is the cylinder pressure and P_T is the exhaust pressure. Several different reference areas can be used. In this paper, the so-called valve curtain area was used as reference area [8]:

$$A_R = \pi D_v L_v \tag{3}$$

where D_v is valve diameter and L_v is the valve lift.

3.1.2. Compression and expansion strokes

During compression and expansion strokes, Eq. (1) can be simplified as:

$$\frac{dT}{d\theta} = \frac{1}{mc_v}\left[-\frac{dQ}{d\theta} - p\frac{dV}{d\theta} + \frac{dm_l}{d\theta}RT\right] \tag{4}$$

where R is the mixture gas constant, θ is the crank angle, c_v is the specific heat at constant volume and $\frac{dm_l}{d\theta}$ is the cylinder mass leakage due to blowby. By neglecting the change in gas constant during compression and expansion the rate of pressure change can be calculated from the ideal gas state equation [8,10]:

$$\frac{dP}{d\theta} = \frac{1}{V}\left[\frac{dm_l}{d\theta}RT + mR\frac{dT}{d\theta} - P\frac{dV}{d\theta}\right] \tag{5}$$

3.1.3. Combustion stroke

Using conservation of mass and energy and the state equations, the rate of cylinder pressure P, unburned and burned gas temperature T_u and T_b are calculated:

$$\begin{aligned}\frac{dP}{d\theta} = {} & \left(\frac{c_{v,u}}{c_{p,u}} - \frac{c_{v,b}}{R_b}\frac{R_u}{c_{p,u}}V_u + \frac{c_{v,b}}{R_b}V\right)^{-1} - \left(1 + \frac{c_{v,b}}{R_b}\right)P\frac{dV}{d\theta} - c_{p,b}T_b \\ & \times \frac{dm_{l,b}}{d\theta} - \frac{R_u}{R_b}c_{p,b}T_u\frac{dm_{l,u}}{d\theta} \\ & - \left[(e_b - e_u) - c_{v,b}\left(T_b - \frac{R_u}{R_b}T_u\right)\right]\frac{dm_b}{d\theta} \\ & + \left(\frac{c_{v,u}}{c_{p,u}} - \frac{c_{v,b}}{R_b}\frac{R_u}{c_{p,u}}\right)\frac{dQ_u}{d\theta} - \frac{dQ}{d\theta}\end{aligned} \tag{6}$$

where subscripts u and b denote unburned and burned properties, respectively, and subscript l, denotes leakage (due to blowby). Also, c_v and c_p are the specific heats at constant volume and pressure, respectively, e is the specific energy and $\frac{dm_b}{d\theta}$ is the mass burning rate, which is derived from a turbulent flame speed model [12]:

$$\frac{dT_u}{d\theta} = \frac{1}{m_u c_{p,u}}\left(V_u\frac{dP}{d\theta} - \frac{dQ_u}{d\theta}\right) \tag{7}$$

$$\begin{aligned}\frac{dT_b}{d\theta} = {} & \frac{P}{m_b R_b}\left[\frac{dV}{d\theta} - \left(\frac{V_b}{m_b} - \frac{V_u}{m_u}\right)\frac{dm_b}{d\theta} + \frac{V_b}{m_b}\frac{dm_{l,b}}{d\theta} + \frac{V_u}{m_u}\frac{dm_{l,u}}{d\theta}\right. \\ & \left. + \left(\frac{V}{P} - \frac{R_u V_u}{c_{p,u}P}\right)\frac{dP}{d\theta} + \frac{R_u}{c_{p,u}P}\frac{dQ_u}{d\theta}\right]\end{aligned} \tag{8}$$

In this paper, the following equation is used for mass burning rate:

$$\frac{dm_b}{d\theta} = \rho_u A_f u_t \tag{9}$$

where ρ is the density, A_f is the flame front area and u_t is the turbulent flame speed.

3.1.4. Fuels laminar flame speed

Since the presented model is predictive, it must evaluate the burn rate of the in-cylinder mixture. The burn rate is completely affected by turbulent flame speed. To calculate turbulent flame speed, laminar flame speed must be determined at first. Various methods for measuring laminar flame speed have been presented up to now for different fuels and air mixtures [8,13–15,17,18]. The applied methods used in this paper are as follows:

3.1.4.1. Hydrogen. Various kinds of formulation for laminar burning velocity of hydrogen/air mixture have been developed. In this paper, Iljima and Takeno's formulation, in which most of important parameters which affect on flame speed such as: equivalence ratio, temperature and pressure, is taken in to account [13,14]. According to Iljima and Takeno's formula, laminar burning velocity of hydrogen/air mixture is as follows:

$$u_l = u_{l0}\left(\frac{T_u}{T_0}\right)^{\alpha_T}\left[1 + \beta_p Log\frac{P}{P_0}\right] \tag{10}$$

where P is the pressure, T_u is the unburned temperature, T_0 = 358 K, P_0 = 0.1 MPa. α_T and β_p are temperature and pressure exponent, respectively:

$$\alpha_T = 1.54 + 0.026(\phi - 1) \tag{11}$$

$$\beta_p = 0.43 + 0.003(\phi - 1) \tag{12}$$

u_{l0}, is the hydrogen laminar burning velocity at 291 K and 1 atm, in m/s, and described by following formula:

$$u_{l0} = 2.98 - (\phi - 1)^2 + 0.32(\phi - 1.70)^3 \tag{13}$$

and ϕ is the equivalence ratio [13,14].

3.1.4.2. Ethanol. Burning velocity of ethanol/air mixture is calculated based on Liao et al's work [15]. According to their research, laminar burning velocity is calculated by the following formula:

$$u_l = u_{l0}\left(\frac{T_u}{T_0}\right)^{\alpha_T}\left[1 + \beta_p Log\frac{P}{P_0}\right] \tag{14}$$

where T_0 = 358 K and P_0 = 0.1 MPa. α_T and β_p are described as follows:

$$\alpha_T = 1.783 - 0.375(\phi - 1) \tag{15}$$

$$\beta_p = \begin{cases} -0.17\sqrt{\phi}\phi \geqslant 1.0 \\ 0.17/\sqrt{\phi}\phi < 1.0 \end{cases} \tag{16}$$

u_{l0}, is the laminar burning velocity of ethanol at 358 K and 1 atm, in m/s:

$$u_{l0} = -2.0707\phi^2 + 4.501\phi - 1.8971 \tag{17}$$

3.1.4.3. Methanol, propane, gasoline. Burning velocity of methanol, propane and gasoline can be calculated from Metghalchi and Keck formulation [8]. Their correlation is defined as follows:

$$u_l = u_{l,0}\left(\frac{T_u}{T_0}\right)^{\alpha}\left(\frac{P}{P_0}\right)^{\beta}(1 - 2.06x_b^{0.77}) \tag{18}$$

where T_0 = 298 K and P_0 = 1 atm are the reference temperature and pressure, and $u_{l,0}$, α and β are functions of equivalence ratio for a given fuel, and x_b is unburned gas diluent fraction. For propane, isooctane and methanol, these constants can be represented as follows:

$$\alpha = 2.18 - 0.8(\phi - 1) \tag{19}$$

$$\beta = -0.16 + 0.22(\phi - 1) \tag{20}$$

$$u_{l,0} = B_m + B_\phi(\phi - \phi_m)^2 \tag{21}$$

where values of ϕ_m, B_m and B_ϕ are as follows: for gasoline, ϕ_m, B_m and B_ϕ are 1.21, 0.305 m/s and −0.549 m/s, respectively, for propane, ϕ_m, B_m and B_ϕ are 1.08, 0.342 m/s and −1.387 m/s, respectively, and for Methane, ϕ_m,B_m and B_ϕ are 1.11, 0.369 m/s and −1.405 m/s, respectively.

3.1.4.4. Methane. Flame speed of methane/air mixture is calculated according to Gu et al. formulation [16]. In their literature, a simple correlation of burning velocities through the empirical expression below was used [17]:

$$u_l = u_{l,0}\left(\frac{T_u}{T_0}\right)^{\alpha_T}\left(\frac{P_u}{P_0}\right)^{\beta_P} \tag{22}$$

The parameters α_T and β_P which depend on ϕ are optimized over the full range of experimental data. The Gu et al. formulation is given by:

$$u_l = \begin{cases} 0.259\left(\frac{T_u}{T_0}\right)^{2.105}\left(\frac{P_u}{P_0}\right)^{-0.504} & \text{if } \phi = 0.8 \\ 0.360\left(\frac{T_u}{T_0}\right)^{1.162}\left(\frac{P_u}{P_0}\right)^{-0.374} & \text{if } \phi = 1.0 \\ 0.314\left(\frac{T_u}{T_0}\right)^{2.000}\left(\frac{P_u}{P_0}\right)^{-0.438} & \text{if } \phi = 1.2 \end{cases} \quad (23)$$

In their research, standard deviations of the difference between experimental and simulation results were 0.008, 0.011, and 0.014 m/s for ϕ = 0.8, 1.0, and 1.2, respectively [16].

3.1.5. Turbulent flame speed

Various methods for describing and calculating the turbulent flame speed have been developed. In this paper "Damkohler and derivatives" method is used [18,19]. According to this model turbulent flame speed is calculated as follows:

$$u_t = u' + u_l \quad (24)$$

where

$$u' = u'_{TDC}\left(1 - 0.5\frac{\theta - 360}{45}\right) \quad (25)$$

$$u'_{TDC} = 0.75\overline{U}_P \quad (26)$$

θ is the crank angle (360 at TDC) and $\overline{U}_P$ is the mean piston speed.

4. Model validation

In order to validate the developed model for all desired fuels, several experiments were conducted. And several diagrams for in-cylinder pressure (Pa) versus crank shaft position (crank angle) and NOx concentration were achieved for each one of the fuels in a

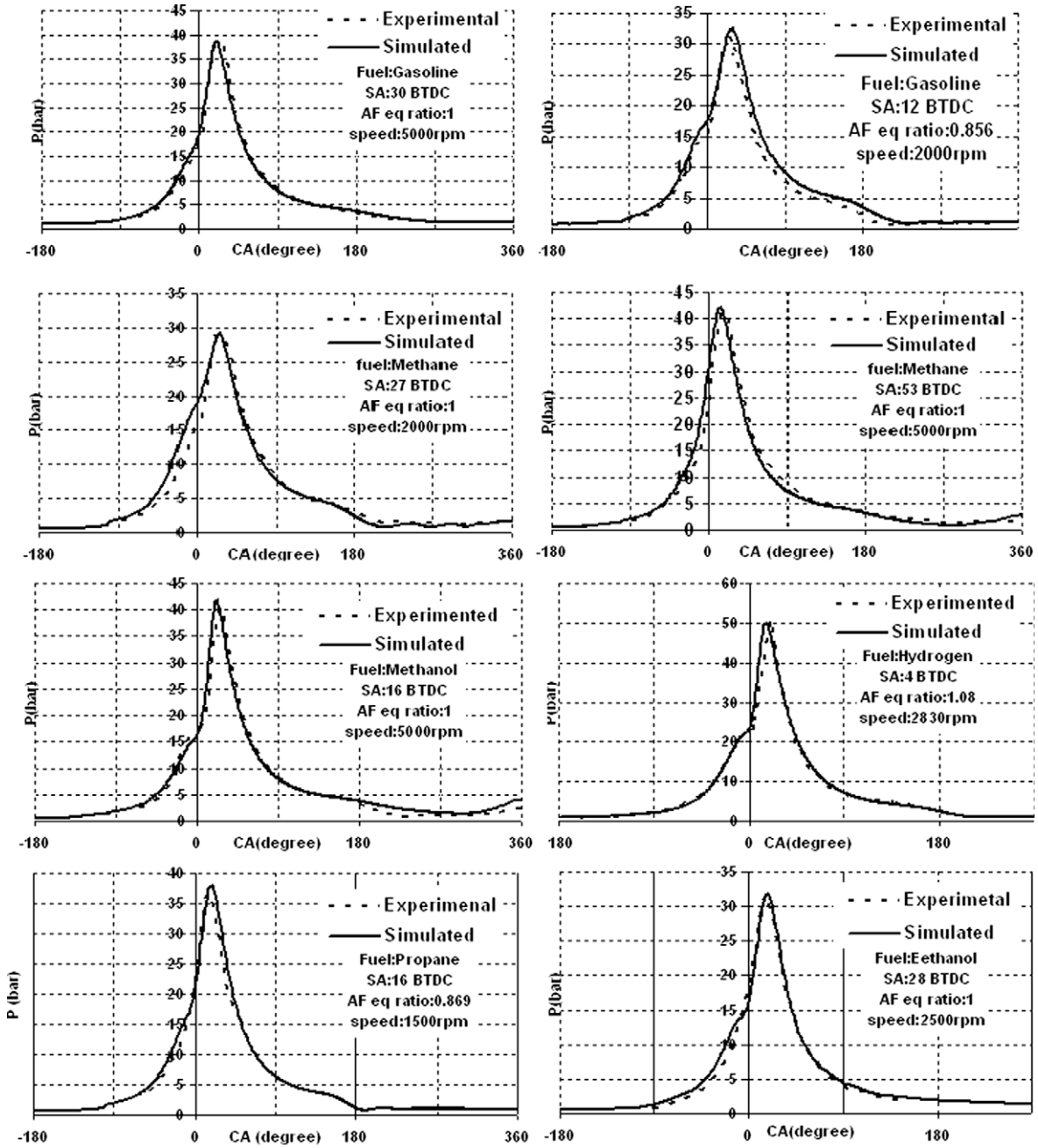

Fig. 2. In-cylinder pressure versus crank angle position comparison between experimental and simulated data.

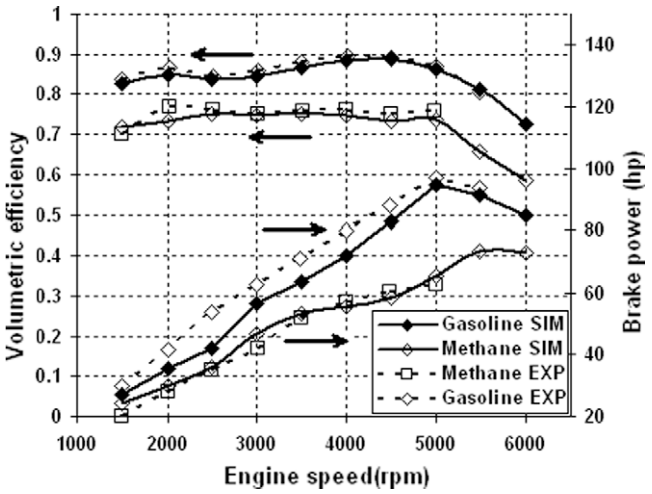

Fig. 3. Simulated and experimental results comparison.

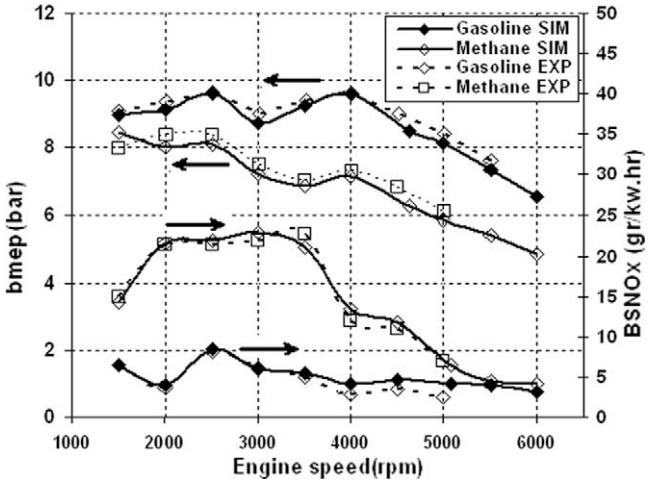

Fig. 4. Simulated and experimental results comparison.

wide range of engine operating conditions. Experimental data were compared with the simulation results. Propane, ethanol and hydrogen were not tested in presented experiment. For validating model for ethanol, hydrogen and propane, some experimental works studied and the model calibrated in order to match them [2,5,20]. In Fig. 2 the in-cylinder pressure variation versus crank angle for different fuels are shown. In Figs. 3 and 4, model ability for predicting engine performance and emissions characteristics, including volumetric efficiency, brake power, brake mean effective pressure and brake specific NOx is checked. Simulation results and experimental data are compared for gasoline and methane.

5. Engine performance and emission

SI engine performance and emission characteristics are directly affected by the type of fuel. These characteristics include: power, torque, brake mean effective pressure, brake specific fuel consumption, brake specific NOx and produced CO.

5.1. Volumetric efficiency and power

Power and torque mainly depend on an engine's in-cylinder mixture mass. Therefore volumetric efficiency plays one of the most important roles among the other engine parameters. In Fig. 5, engine volumetric efficiency and brake power are shown for different fuels. Near the engine speed of 4500 volumetric efficiency reaches to its maximum peak and then decreases because of high pressure loss and choking in high engine speeds. As liquid fuels have latent heat of vaporization, they produce a cooling effect on intake charge during vaporization. Therefore, there will be an increase in intake mixture density and consequently in volumetric efficiency, but gaseous fuels which are vapor in ambient temperature, not only have no cooling effect, but also cause a decrease in volumetric efficiency, due to larger volume of fuel in inlet mixture. As expected, it can be seen in Fig. 4 that engine has the minimum volumetric efficiency when fueled with hydrogen and methane. Stoichiometric A/F ratio is another important parameter that affects volumetric efficiency. When stoichiometric A/F ratio is low that means there is more injected fuel in inlet air and results in decreasing volumetric efficiency. Gasoline has the highest volumetric efficiency because of high stoichiometric A/F ratio (14.6) and high latent heat of vaporization. In Table 1, it is seen that latent heat of vaporization of methanol is higher than other fuels but volumetric efficiency of methanol fueled engine is less than gasoline. The reason is that methanol has the smallest stoichiometric A/F ratio. The engine operating on methane, methanol, hydrogen, propane and ethanol will experience an average reduction in volumetric efficiency by 12%, 5%, 28%, 10% and 8% comparing to gasoline, respectively. It can be seen that engine produce less power when operating on methane and hydrogen. As mentioned before, this is because of lower volumetric efficiency of methane and hydrogen fueled engine. In order to regain that lost power, two methods can be used. Turbo-charging and/or raising the compression ratio under naturally aspirated operation. Engine maximum power for all of the fuels happens between 4500 and 5500 rpm. Although the engine volumetric efficiency fueled with hydrogen is lower than that of methane. But power produced by hydrogen is higher. That is because of higher heating value of hydrogen. The power produced by methane, methanol, hydrogen, propane and ethanol is less of gasoline by 20%, 13%, 19%, 10% and 10%, respectively. As the engine is designed for operating on gasoline, more power is obtained when gasoline is applied. All the other fuels have a higher octane number than gasoline, so engine compression ratio could be higher if the engine was dedicated to those fuels, and therefore engine performance could be improved.

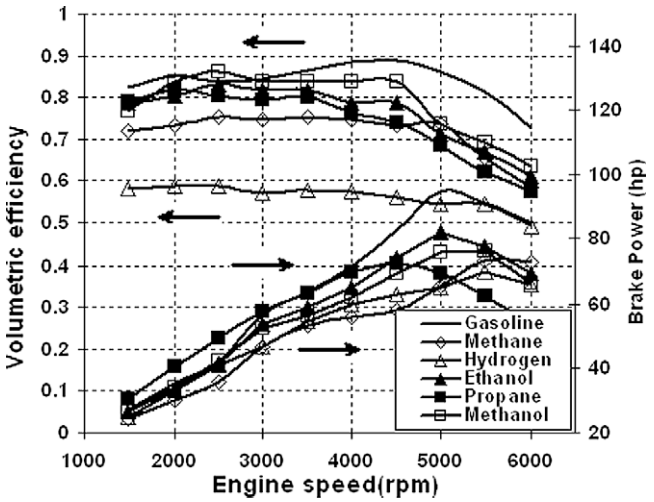

Fig. 5. Variation of volumetric efficiency and bake power with different fuels versus engine speed.

5.2. Break mean effective pressure

Fig. 6 presents a comparison between brake mean effective pressures (BMEP) of different fuels. For naturally aspirated spark ignition engines, maximum values for BMEP are in the range 850–1050 kPa at the engine speed where maximum torque is obtained. At the speed where maximum power occurred, BMEP values are 10–15% lower. The variation of BMEP and brake power is primarily due to the variation in volumetric efficiency [8]. In Fig. 6, it can be seen that the shape and trend of BMEP curve follows the volumetric efficiency curve. The reduction in BMEP with methane operation is seen through out the speed range. Part of this BMEP loss is due to longer ignition delay and lower flame speed of methane. In more spark advance, combustion starts earlier with respect to TDC and there is a greater amount of negative work done on the piston before TDC compared to gasoline. The remainder of the BMEP loss is due to the lower volumetric efficiency.

5.3. Break specific fuel consumption

Brake specific fuel consumptions (BSFC) for different fuels are compared in Fig. 7. BSFC is a function of heating value of fuel, spark timing, *A*/*F* ratio, engine load and speed. As the engine speed raises the BSFC rises as well. It is mostly due to the more working cycles in a specific period of time at high engine speeds [8,10]. In Fig. 7, BSFC of methanol is the highest followed by ethanol. BSFC of Methanol and ethanol fueled engine is more than gasoline by 91% and 49%, respectively. The reason is that heating value and stoichiometric air/fuel ratio are the smallest for these two fuels which means, for specific air/fuel equivalence ratio, more fuel is needed. BSFC of methane has been measured 8% lower than gasoline. The reason is that methane heating value is higher than gasoline. Therefore a specified amount of heat can be released with less amount of fuel. The BSFC of propane fueled engine is approximately 9% less than gasoline. As expected, because of the highest heating value and highest stoichiometric air/fuel ratio, the engine has the lowest BSFC when fueled by hydrogen.

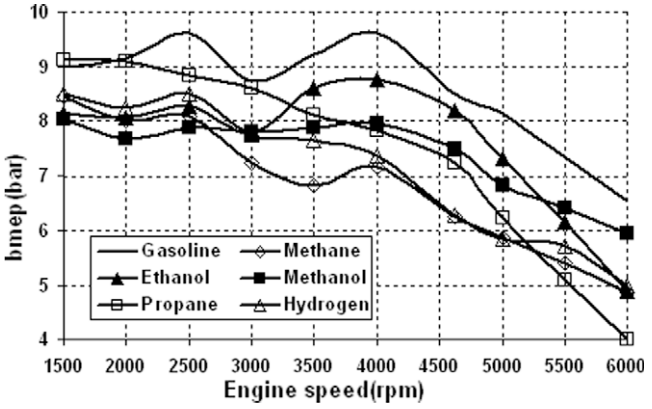

Fig. 6. Variation of brake mean effective pressure versus engine speed for different fuels.

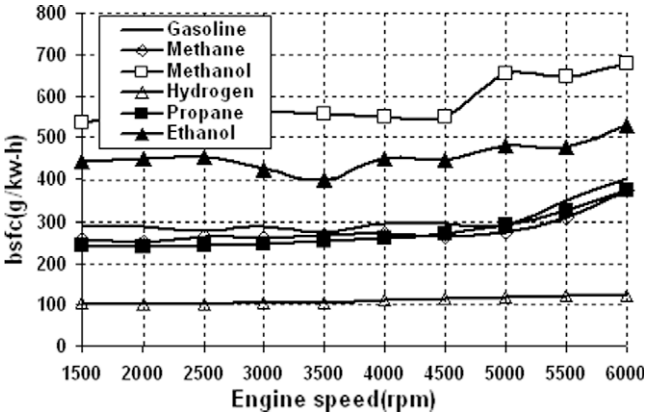

Fig. 7. Variation of brake specific fuel consumption versus engine speed for different fuels.

5.4. Brake specific NOx

In Fig. 8 brake specific NOx (BSNOx) for different fuels is compared. According to measured and predicted data hydrogen and methane cause more BSNOx. It must be remembered that NOx formation takes place at high temperatures and the increase of BSNOx is caused by higher combustion temperature of hydrogen and methane.

There are two main reasons for this increase in temperature. Firstly, as noted, for gaseous fuels there is no cooling effect which will cause a higher initial temperature for in-cylinder charge. Secondly, which is the case for methane, more spark advance is needed because of the low flame speed of methane which rises peak of combustion temperature and pressure. In Fig. 8, it is seen that NOx emitted by hydrogen fueled engine is rising steadily as the engine speed increases and it does not match with experimental results. The error is due to using Woschni heat transfer model which is not proper for hydrogen [14]. Since there is no better alternative model, using Woschni model is inevitable [14]. Also it must be mentioned that hydrogen fueled engine is tested at stoichiometric mixture condition and the value of NOx in that situation is dramatically high. It is clear that hydrogen can perform on much lower equivalence ratio which results in a really lower NOx value in comparison to stoichiometric condition.

Methanol and ethanol have the lowest heating value. Methanol flame speed is the highest after of hydrogen, therefore a lower spark advance is used and combustion temperature is lowered. So BSNOx produced by methanol is less than the other fuels (NOx emitted by methanol fueled engine is 53% less than the gasoline fueled engine).

5.5. CO concentration

In Fig. 9, CO concentration is shown for different fuel and air mixtures. CO concentration in exhaust gases mostly depends on air/fuel ratio. A rich mixture causes more CO in exhaust gases

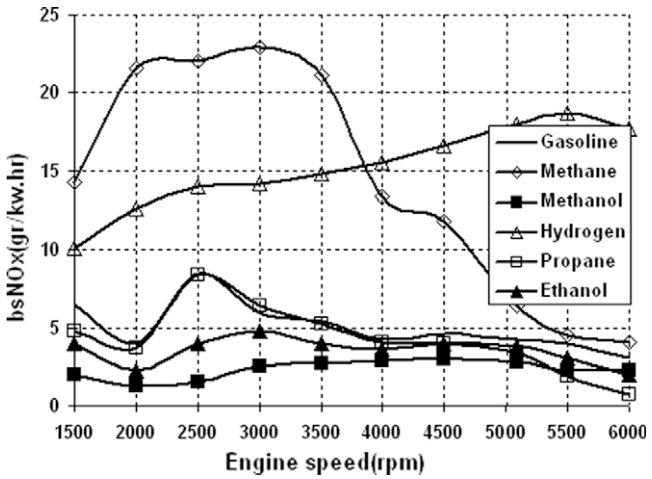

Fig. 8. Variation of brake specific NOx versus engine speed for different fuels.

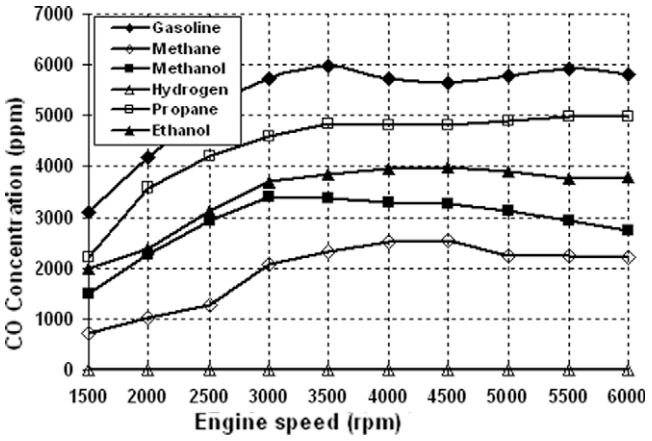

Fig. 9. Variation of CO concentration versus engine speed for different fuels.

[8,10]. The more the operating condition is close to the stoichiometric point, the less amount of CO is produced. Carbon to hydrogen ratio of fuel (C/H ratio) is another parameter which affects the formation of CO. It is obvious that no CO is produced in hydrogen combustion, as there is no atom of carbon in hydrogen's structure, but due to a lubricant oil leakage flow from outside to inside of the cylinder, a CO formation is anticipated when engine is operating with this fuel.

6. Conclusions

Performance and emissions characteristics of a four-stroke, four-cylinder engine were experimentally measured for gasoline, methane and methanol.

A computer code was developed in Matlab environment which enables to simulate SI engine performance and emissions characteristics fueled by methane, gasoline, methanol, propane, ethanol and hydrogen. Then simulation results were validated by experimental data and previous literatures. Finally a detailed comparison between measured and predicted performance and emissions characteristics was carried out.

Gaseous fuels which are investigated in this paper have common properties that provide them some advantages and disadvantages relative to conventional liquid fuels. They can be used with higher compression ratios. Gaseous fuels decrease volumetric efficiency and increase combustion temperature which results in increase of BSNOx. Application of gaseous fuel in a gasoline engine generally has the disadvantage of reduced power, due to lower volumetric efficiency. To obviate this shortcoming, one can raise engine compression ratio or make use of a turbo charger to increase volumetric efficiency.

Liquid fuels tested in presented paper, produce more power rather than gaseous fuels and they produce less NOx. Brake specific fuel consumption of engine, operating on hydrogen, propane and methane is less than that of gasoline while BSFC of methanol is nearly two times of gasoline.

More CO is produced when engine is performed with gasoline it is due to smaller H/C ratio, while CO production of hydrogen fueled engine is very low.

For gaining high performance and low emission, engine should be dedicatedly designed for each one of the fuels. In a dual-fuel or flexible-fuel engine, some performance properties might be sacrificed.

References

[1] Verhelst S, Maesschalck P, Rombaut N, Sierens R. Efficiency comparison between hydrogen and gasoline, on a bi-fuel hydrogen/gasoline engine. Int J Hydrogen Energy 2009;34:2504–10.
[2] Bayraktar Hakan, Durgun Orhan. Investigating the effects of LPG on spark ignition engine combustion and performance. Energy Conver Manage 2005;46:2317–33.
[3] Mustafi NN, Miraglia YC, Raine RR, Bansal PK, Elder ST. Spark-ignition engine performance with 'Power-gas' fuel (mixture of CO/H2): a comparison with gasoline and natural gas. Fuel 2006;85:1605–12.
[4] Shamekhi A, Khtibzade N, Shamekhi AH. Performance and emissions characteristics of a bi-fuel SI engine fueled by CNG and gasoline. ASME paper, ICES2006-1387; 2006.
[5] Cavalcante Cordeiro de Melo T, Bastos Machado G, Machado RT, Pereira Belchior Jr CR, Pereira PP. Thermodynamic modeling of compression, combustion and expansion processes of gasoline, ethanol and natural gas with experimental validation on a flexible fuel engine. SAE World Congress, 2007-24-0035; 2007.
[6] Verhelst S, Sierens R, Verstraeten S. Development of a simulation code for hydrogen fuelled SI engines. ASME paper, ICES2006-1317; 2006.
[7] Schoenung Susan M. Hydrogen vehicle fueling alternatives: an analysis developed for the international energy agency. SAE World Congress, 2001-01-2528; 2001.
[8] Heywood JB. Internal combustion engines fundamentals. New York: McGraw-Hill; 1988.
[9] Woschni G. A universally applicable equation for the instantaneous heat transfer coefficient in the in the internal combustion engine. SAE World Congress, 670931; 1967.
[10] Ferguson Colin R, Kirkpatrick Allan T. Internal combustion engines: applied thermoscience. 2nd ed. John Wiley and Sons, Inc.; 2001.
[11] Shamekhi AH. Simulation and fuzzy spark advance control in si engines by ion current sensing. PhD Thesis, Department of Mechanical Engineering, K.N. Toosi University of Technology; September 2004.
[12] Horlock F.R.S. JH, Winterbone DE. The thermodynamics and gas dynamics of internal combustion engines, vol. II. Oxford: Clarendon Press; 1986.
[13] Iljima T, Takeno T. Effects of temperature and pressure on burning velocity. Combust Flame 1986;65:35–43.
[14] Salimi Farhad, Shamekhi Amir H, Pourkhesalian Ali M. Effect of spark advance, A/F ratio and valve timing on emission and performance characteristics of hydrogen internal combustion engine, SAE World Congress, 2009-01-1424; 2009.
[15] Liao SY, Jiang DM, Huang ZH, Zeng K, Cheng Q. Determination of the laminar burning velocities for mixtures of ethanol and air at elevated temperatures. Appl Thermal Eng 2007;27:374–80.
[16] Gu XJ, Haq MZ, Lawes M, Woolley R. Laminar burning velocity and markstein lengths of methane–air mixtures. Combust Flame 2000;121:41–58.
[17] Metghalchi M, Keck JC. Laminar burning velocity of iso-octane-air, methane-air and methanol-air at high temperature and pressure. In: Proceedings of the eastern section of the combustion institute, Hartford, Conn; November 1977.
[18] Verhelst S. A study of the combustion in hydrogen-fuelled internal combustion engines, PhD thesis, Ghent University, Gent, Belgium; 2005.
[19] Hall MJ, Bracco FV. A study of velocities and turbulence intensities measured in firing and motored engines. SAE World Congress, 870453; 1987.
[20] Swain Michael R, Schade Gregory J, Swain Matthew N. Design and testing of a dedicated hydrogen-fueled engine, SAE World Congress, 961077; 1996.